Biochemical and Biophysical Research Communications 431 (2013) 706–711

Contents lists available at SciVerse ScienceDirect

Biochemical and Biophysical Research Communications

journal homepage: www.elsevier.com/locate/ybbrc

The Gly–Ala repeat modulates the interaction of Epstein–Barr virus nuclear antigen-1 with cellular chromatin

Giuseppe Coppotelli *[,1,2], Nouman Mughal [2], Maria G. Masucci *

Department of Cell and Molecular Biology, Karolinska Institutet, S-17177 Stockholm, Sweden

ARTICLE INFO

Article history:
Received 10 January 2013
Available online 21 January 2013

Keywords:
EBV
EBNA1
AT-hook
HMGA proteins
Gly–Ala repeat

ABSTRACT

The Epstein–Barr virus (EBV) nuclear antigen-1 (EBNA1) plays a pivotal role in EBV infection by anchoring the viral episome to cellular DNA, which regulates replication and partitioning in dividing cells. Here, we have used fluorescence recovery after photobleaching (FRAP) and fluorescence loss in photobleaching (FLIP) techniques to study the interaction of EBNA1 with cellular chromatin in interphase and mitosis. This analysis revealed that while EBNA1 is highly mobile in both conditions, mobility is significantly reduced in mitosis when an immobile fraction is also detected. The N-terminal chromatin-targeting module of EBNA1 includes two Gly–Arg rich domains (GR1 and GR2) separated by a Gly–Ala repeat (GAr) of variable length. Using a set of deletion mutants and GFP-fusion reporters, we found that the GR domains cooperatively determine the mobility of EBNA1, whereas mobility is increased by the interposed GAr in a length-dependent manner. These findings highlight a previously unrecognized property of the interaction of EBNA1 with cellular chromatin that may fine-tune its function in the maintenance of viral latency.

1. Introduction

Epstein–Barr virus (EBV) is a gamma herpesvirus widely spread in humans that can immortalize B-lymphocytes *in vitro* and *in vivo*. EBV infection is associated with a variety of malignancies, including Burkitt's lymphoma, Hodgkin's disease, nasopharyngeal carcinoma and post-transplant lymphoproliferative disorders in immunosuppressed patients [1]. Similar to other herpesviruses, EBV persists for life in healthy carriers by colonizing a cellular reservoir where only few latency-associated genes are expressed [2]. The establishment of latency in the proliferative B-cell compartment is dependent on expression the EBV nuclear antigen-1 (EBNA1) that acts as a genome maintenance protein by coordinating the replication of the viral and cellular genomes, and the correct partitioning of the viral genome in daughter cells [3]. This function of EBNA1 is dependent on two protein domains located at the opposite ends of the molecule that interact with the viral origin of plasmid replication, *OriP*, and with cellular chromatin, respectively.

The interaction of EBNA1 with the viral *OriP* has been extensively studied. EBNA1 homodimers bind to the region in two repetitive clusters: the family of repeat (FR) and the dyad symmetry element (DS), that contain 20 and 4 high-affinity binding sites, respectively [4]. In contrast, the mode and regulation of the interaction of EBNA1 with cellular chromatin is still poorly understood. Binding to mitotic chromosomes occurs via two N-terminal linking regions, LR1 and LR2, [5–7] that are spaced by a Gly–Ala repeat (GAr) of variable length in different EBV isolates [8]. The GAr is not essential for B-cell immortalization *in vitro* but was shown to regulate EBNA1 mRNA translation [9] and protein stability [10]. The linking regions hereafter referred to as GR1 and GR2, are characterized by reiterations of the Arg–Gly–Arg (RGR) peptide, which is found in several DNA or RNA binding proteins. Short RGR motifs are also present in the AT-hook of High Mobility Group A (HMGA) proteins. The AT-hook binds to the minor groove of AT-reach DNA [11] at sites partially overlapping with the binding sites of linker histones [12]. The mode of interaction of EBNA1 with cellular DNA is still actively debated. The chromatin-anchoring module of the viral protein can be replaced with either the AT-hooks of HMGAs or by histone H1 without significant effects on the replication or partitioning of the viral episome [13]. Furthermore, purified GR1 and GR2 peptides were shown to bind to AT-rich DNA *in vitro* [7], and fusion to the juxtaposed GR1 and GR2 tethered a cytosolic protein to cellular chromatin [14], suggesting that EBNA1 may directly interact with DNA. However, EBNA1 also interacts with several DNA-binding proteins that are likely to contribute to, and may even mediate the binding to chromatin.

While the interaction of EBNA1 to mitotic chromosomes is relatively well understood, the association with chromatin during

* Corresponding authors. Address: CMB, Karolinska Institutet, Box 285, 17177 Stockholm, Sweden.
E-mail address: maria.masucci@ki.se (M.G. Masucci).
[1] Current address: Department of Neuroscience, Karolinska Institutet, 17177 Stockholm, Sweden.
[2] The authors contributed equally to this work.

0006-291X/$ - see front matter © 2013 Elsevier Inc. All rights reserved.
http://dx.doi.org/10.1016/j.bbrc.2013.01.054

interphase and the purpose of such interaction are less clear. We have shown that EBNA1 is capable of detergent resistant interaction with chromatin during interphase and such interaction is partially responsible for the long half-life of the protein [14]. Using ChipSeq analysis Lu et al. have found that EBNA1 interacts, either directly or indirectly, with a large number of cellular genes and chromosomal loci [15]. More recently, using Fluorescence recovery after photobleaching (FRAP) and fluorescence resonance energy transfer (FRET) techniques, Jourdan et al. have confirmed the interaction of EBNA1 with both interphase and mitotic chromatin and shown that the interaction is modulated by binding to high Mobility Group B protein-2 (HMGB2) [16]. However, silencing of HMGB2 in the EBV positive Raji cell line had no effect on episome replication, partitioning and stability, suggesting that the interaction is not essential for the loading of EBNA1 on chromatin.

In this study we sought to identify structural features of EBNA1 that may influence the binding to cellular chromatin. Using live-cell imaging techniques, we found that a highly dynamic interaction of EBNA1 with cellular chromatin is dependent on the cooperative effect of the GR1 and GR2 domains and is modulated by the length of the intervening GAr.

2. Materials and methods

2.1. Antibodies and reagents

Affinity purified rabbit anti-EBNA1 antibody K67.3 was a gift from J. Middeldorp (Vrije Universiteit, Amsterdam, Holland). Rabbit anti-GFP, horseradish peroxidase conjugated donkey anti-Rabbit lgG and TRITC-conjugated mouse anti-rabbit antibodies were from Santa Cruz Biotechnology Inc. (Santa Cruz, CA, USA), GE Healthcare Biosciences (Pittsburgh, PA, USA) and DAKO (Glostrup, DK), respectively. KaryoMAX® Colcemid™ Solution was purchased from Gibco Life Technologies (Grand Island, NY, USA).

2.2. Cell lines and transfection

The human osteosarcoma cell line U2OS and the EBV positive nasopharyngeal carcinoma cell line C666-1 were cultured in Iscove's Modified Dulbecco's Medium (IMDM) supplemented with 10% Fetal Bovine Serum (FBS), 2 mM Glutamine and 10 μg/ml Ciprofloxacin (all from Sigma–Aldrich, St. Louis, MO, USA). Semi-confluent cell monolayers grown on plastic dishes or glass cover slides (VWR International, Radnor PA, USA) were transfected with the jet-PEI® transfection kit (Polyplus Transfection, Illkirch, France).

2.3. Plasmids

The pFLAG-EBNA1 and GFP-EBNA1 expression vectors [13] were kindly provided by Kieff (Harvard Medical School, Boston MA). Plasmids encoding GFP-NLS [17], GFP-H1.0, GFP-HMGA1a, GFP-EBNA1-ΔGA and GFP-EBNA1-DBD [18] were described previously. The p3xFLAG-GR1/2GFP plasmid was generated by inserting the GFP coding sequence amplified with the primer pair: fw-AAACTCGAGATGGTGAGCAAGGGCGAGGAGC, rev-TTTGCGGCCGCTT ACTTGTACAGCTCGTCCATGCCGAG in the *Xho*I/*Not*I sites of p3xFLAG-GR1/2-NLS-VK [19]. p3xFLAG-GR1-GA25GFP was generated by replacing the VK fragment in the *Hin*dIII/*Sal*I sites of p3xFLAG-VKGA25 [19] with the GR1 sequence amplified with the primers pair: fw-AAAAAGCTTTTAACACGTGCTGCAGATG CG and rev-AAAGTCGACCTGCTCCTGTTCCACCGTGGGT. p3xFLAG-GR1/2GA25GFP was generated by cloning the GR2-GFP fragment amplified from p3xFLAG-GR1/2-GFP with the primers pair: fw-AAAG GATCCGGAGGTGGAGG CCGGGGTCGA and rev-TTTGCGGCCGCT TACTTGTACAGCTCGTCCATGCC GAG in the *Bam*HI/*Not*I sites of p3xFLAG-GR1-GA25. p3xFLAG-GR1/2GA75GFP was generated by inserting two *Bgl*II/*Bam*HI GA25 fragments [19] in the *Bam*HI site of p3xFLAG-GR1/2GA25GFP. p3xFLAG-GR1-GFP and p3xFLAG-GR2-GFP were generated by ligating PCR products encoding EBNA1 amino acid 38–89 and 325–377, generated with the primer pairs: fw-AAAAAGCTTAACCATGGACGAGGACGGG GAAGAGG, rev-CATCTCGAGTCCTGTTCCACCGTGGGCCCCTTT and fw-AA AAAGCTT GGAGGTGGAGGCCGGGGTCGAGG, rev-CATCTCGAGACCACGT CCAC GACCTCTCCCCCTGGC, in the *Hin*dIII/*Xho*I of p3xFLAG-GR1/2-GFP.

2.4. Immunofluorescence

Cells grown on cover slides were fixed with 4% formaldehyde in PBS for 20 min followed by permeabilization and blocking for 30 min in PBS containing 1% Triton® X-100 and 3% w/v BSA. For detection of EBNA1, the slides were incubated for 1 h at room temperature with the K67.1 antibody (1:1000) followed by TRITC-conjugated anti-rabbit IgG antibody (1:100). The slides were mounted with VECTASHIELD medium containing DAPI (Vector Laboratories Inc. Burlingome, CA). Digital images were captured using a LEITZ-BMRB fluorescence microscope (Leica, Wetzlar, Germany) equipped with a CCD camera (Hamamatsu Photonics KK, Tokyo, Japan) and analyzed with ImageJ 1.45S software National Institutes of Health (NIH) (Bethesda, MD).

2.5. Western Blot

Cell lysates were prepared in RIPA buffer (150 mM TRIS–HCl pH 7.5, 150 mM NaCl, 2 mM EDTA, 1% Triton, 0.1% SDS and protease inhibitors) and protein concentration was measured using the BIO-RAD Dc protein assay kit (BIORAD Laboratories, Hercules, CA). Twenty μg of proteins were fractionated in NUPAGE® Novex® Bis-Tris precast gels (Life Technologies Corporation, Grand Island, NY) and blotted on 0.2 μm nitrocellulose membranes (Amersham Hybond ECL, GE Helthcare, Buckinghamshire, UK). After incubation with the indicated primary and secondary antibodies, immunocomplexes were detected by chemiluminescence (PIERCE® ECL, Thermo Scientific, Rockford, IL).

2.6. Fluorescence recovery after photobleaching (FRAP) and fluorescence loss in photobleaching (FLIP)

FRAP experiments were performed 48 h after transfection using a Zeiss LSM 510 META confocal microscope equipped with a CO_2 chamber. Thirty pre-bleach images were acquired using a Plan-Apochromat 63x/1.4 Oil Dic objective zoom 8, followed by a 5 iterations bleach pulse in a strip region of 1.74 × 1.4 μm. Six hundred imagines were acquired with a scan speed of 38.4 ms/cycle and a delay of 5 ms. The power of a 25 mW argon laser (488 nm line) was set to 0.1% for imaging and to 100% for bleaching. FRAP recovery curves were generated by normalizing the fluorescence intensity in the bleached area to the initial fluorescence in the same area. A least 10 cells were analysed in each experiment. The half-time recovery ($t_{1/2}$) was calculated by fitting the curves with the Prism5 software (GraphPad Software Inc, La Jolla CA, USA), using non-linear regression and One-phase association equations. For FLIP experiments, a rectangular region of 15 × 5 μm within the nucleus was repeatedly bleached with a 488 nm laser line (100% output) using a Zeiss LSM510 META with Plan-Apochromat 63x/1.4 Oil Dic objective zoom 6. Five images were recorded before bleaching and a total of 170 images were acquired with a scan speed of 1.57 s/cycle and a cycle delay of 1 s. The fluorescence intensities were normalized to the initial fluorescence.

2.7. Statistical analysis

Statistical analysis was performed by *t*-test. Significant probabilities are indicated as: $p < 0.05$ (*), $p < 0.01$ (**) and $p < 0.001$ (***).

3. Results

3.1. EBNA1 establishes a dynamic interaction with cellular chromatin in interphase and mitosis

Fluorescence loss in photobleaching (FLIP) and Fluorescence recovery after photobleaching (FRAP) are powerful techniques to study the dynamics of protein–protein and protein-nucleic acid interaction in living cells. We used therefore FLIP and FRAP to investigate the mobility of GFP-tagged EBNA1 in transfected U2OS cells. As reference, the mobility of EBNA1 was compare to that of GFP-tagged High Mobility Group A protein-1a (GFP-HMGA1a) and histone H1 (GFP-H1.0) that are known to exhibit high and intermediate mobility, respectively. The mobility of GFP-EBNA1 was close to that of HMGA1a in FLIP (Fig. 1A and B) and FRAP (Fig. 1C) assays. The half-time of fluorescence loss measured in FLIP was approximately 91.44 s for EBNA1 and 60.35 s for HMGA1a (Fig. 1B), while the half-time recovery measured in FRAP was 4.43 ± 0.28 s and 0.86 ± 0.02 s, respectively (Fig. 1C). Both proteins were highly mobile compared to histone H1.0 that needed more than 25 s for the half-time fluorescence recovery in FRAP (Fig. 1C) and over 600 s for half-time fluoresce loss in FLIP (Fig. 1B).

EBV positive cells may carry up to several hundred copies of the viral episome. In order to investigate whether the mobility of EBNA1 is influenced by the presence of multiple viral episomes, the analysis was repeated in the EBV positive nasopharyngeal carcinoma cell line C666-1. As illustrated by the representative experiment shown in Fig. 1D, FRAP analysis in GFP-EBNA1 transfected C666-1 and U2OS cells did not reveal significant differences in the kinetics of fluorescence recovery, indicating that the interaction of EBNA1 with cellular DNA is not affected by the viral episomes. Notably, a comparable recovery of fluorescence was observed in cells expressing GFP-NLS and GFP-EBNA1, suggesting that the entire pool of EBNA1 is mobile in interphase cells.

We then tested whether the mobility of EBNA1 may change in mitosis when a more stable interaction with cellular chromatin could be required to anchor the episomes to the migrating chromosomes. To this end, the FRAP recovery curves of GFP-EBNA1 were compared in transfected U2OS cells during interphase or in cells arrested in mitosis by treatment with colcemide (Fig. 2A). We observed a significant difference in the kinetics of fluorescence recovery in interphase and mitotic cells with half-time recoveries of 4.7 ± 0.14 s and 9.53 ± 0.39 s, respectively (Fig. 2B). Furthermore, in mitotic cells a significant proportion of GFP-EBNA1 fluorescence did not recover after 25 s, when the curve had almost reached plateau. By extrapolating the FRAP recovery curve in repeated experiments, we calculated that approximately 20% of the protein has a recovery time in excess of 1 min, and at least a portion of this is likely to be immobile during mitosis.

3.2. The interaction of EBNA1 with cellular chromatin is modulated by the Gly–Ala and Gly–Arg repeats

The chromatin targeting modules encoded in the GR1 and GR2 domains of EBNA1 are separated by a GAr domain of variable length [8]. In order to investigate whether this structural organization influences the interaction of EBNA1 with cellular chromatin,

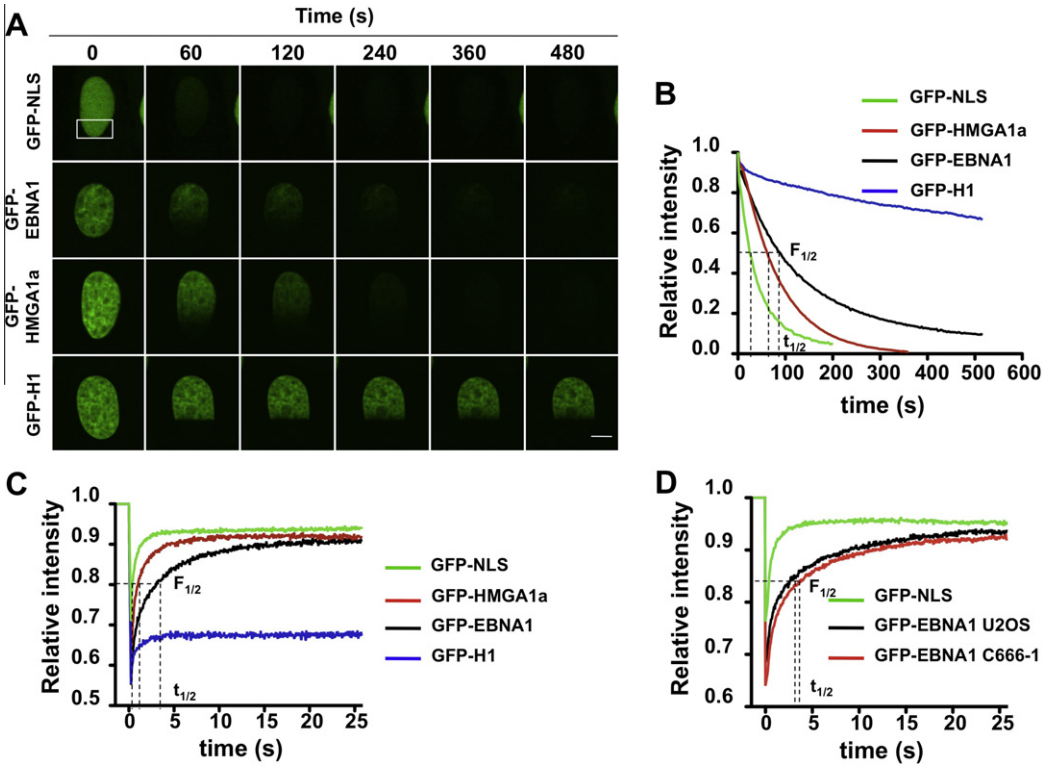

Fig. 1. EBNA1 is highly mobile on interphase chromatin. The mobility of the indicated GFP fusion proteins in transfected U2OS and C666-1 cells was measured in FLIP and FRAP assays. (A) Representative micrographs illustrating the loss of GFP fluorescence in FLIP assays. (B) The FLIP kinetics was recorded in at least 10 cells per each condition in three independent experiments. $F_{1/2}$ was calculated as (initial Fluorescence + final Fluorescence)/2. (C) The FRAP kinetics was recorded in at least 10 cells per each condition in three independent experiments. $F_{1/2}$ was calculated as (Fluorescence recovered – Fluorescence post bleaching)/2. The $t_{1/2}$ required for 50% fluorescence loss ($F_{1/2}$) was calculated by fitting the curve with Prism5 using non-linear regression and One-phase association equation. The $t_{1/2}$ for GFP-NLS, GFP-HMGA1a, GFP-EBNA1 and GFP-H1 were: 0.26 ± 0.02 s, 0.86 ± 0.02 s, 4.43 ± 0.28 s and >25 s, respectively. (D) Comparison of the FRAP kinetics in U2OS and in the EBV positive C666-1 cells illustrating the lack of effect of viral episomes on the mobility of EBNA1.

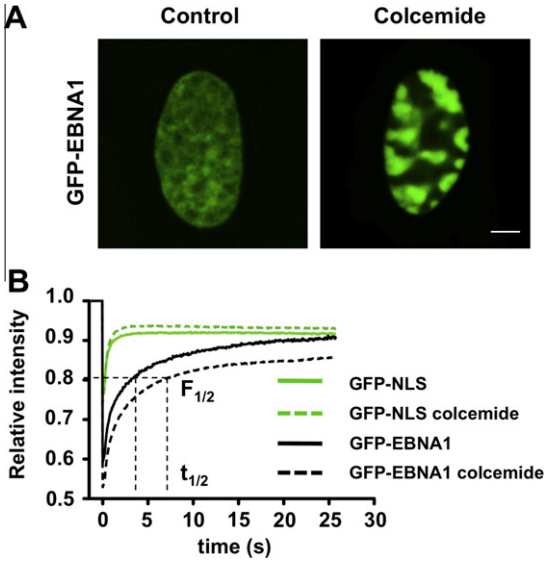

Fig. 2. The mobility of EBNA1 is reduced on metaphase chromosomes. (A) Representative micrographs illustrating the localization of EBNA1 in interphase and metaphase nuclei. Transfected U2OS cells were arrested in metaphase by treatment with 10 μg/ml of colcemide for 12 h. Scale bar 5 μm. (B) FRAP kinetics of GFP-NLS and GFP-EBNA1 in interphase and metaphase arrested cells. The fluorescence recovery was significantly slower in mitotic compare to interphase cells, $t_{1/2}$: 4.7 ± 0.14 s and 9.53 ± 0.39 s, respectively.

the mobility of GFP-EBNA1 was compared with that of deletion mutants lacking either the GAr alone (GFP-EBNA1-ΔGA) or the entire N-terminal domain (GFP-DBD) (Fig. 3A). As expected, deletion of the N-terminus abolished the ability of GFP-DBD to interact with cellular chromatin resulting in half-time fluorescence loss in FLIP (Fig. 3B and C) and half-time fluorescence recovery in FRAP (Fig. 3D) comparable to those of the soluble GFP-NLS. In addition, the mobility of EBNA1 was significantly impaired by deletion of the GAr. The half-time fluorescence loss of GFP-EBNA1-ΔGA measured in FLIP increased from 91 s to approximately 226 s (Fig. 3B and C), while the half-time fluorescence recovery measured in FRAP showed an approximately fourfold increase, from 4.43 ± 0.43 s to 16.52 ± 0.28 s ($p < 0.0001$) (Fig. 3D and Table 1).

To better understand the effect of the GR and GAr domains we engineered artificial chromatin-targeting modules where the GR1 and GR2 were fused to GFP either lone (GR1-GFP and GR2-GFP) or in combination without (GR1/2-GFP) or with intervening GAr peptides of increasing length (GR1/2-GA25-GFP and GR1/2-GA75-GFP, Fig. 4A). Analysis of proteins size and localization by western blot and fluorescence microscopy confirmed the expression of nuclear proteins of the expected size (Fig. 4B and C and not shown).

We first asked whether the GR1 and GR2 domains, that are both needed for tethering the episome to cellular chromatin, play an equally important role in regulating protein mobility. To this end, the mobility of GR1/2-GFP was compared to that of GFP chimeras fused to either the first 89 amino acid of EBNA1 (GR1-GFP), or to EBNA1 amino acid 324–376 (GR2-GFP, Fig. 4D). FRAP analysis revealed that, while each of the two modules alone could slightly decrease the mobility of GFP, both modules are needed to achieve a halt-time fluorescence recovery comparable to that of EBNA1 ($t_{1/2}$ = 3.54 ± 0.1 s, Fig. 4D). We then compared the FRAP recovery curves of the GR1/2-GFP chimera with those of chimeric protein where the GR1 and GR2 domains were spaced by GAr peptides of different length. This analysis revealed a direct correlation between protein mobility and the length of the GAr. Thus, the half-time fluorescence recovery of GR1/2-GFP measure in FRAP decreased from 3.54 ± 0.1 s to 2.46 ± 0.07 and 1.23 ± 0.07 s in the GR1/2-GA25-GFP and GR1/2-GA75GFP, respectively (Fig. 4E and Table 2).

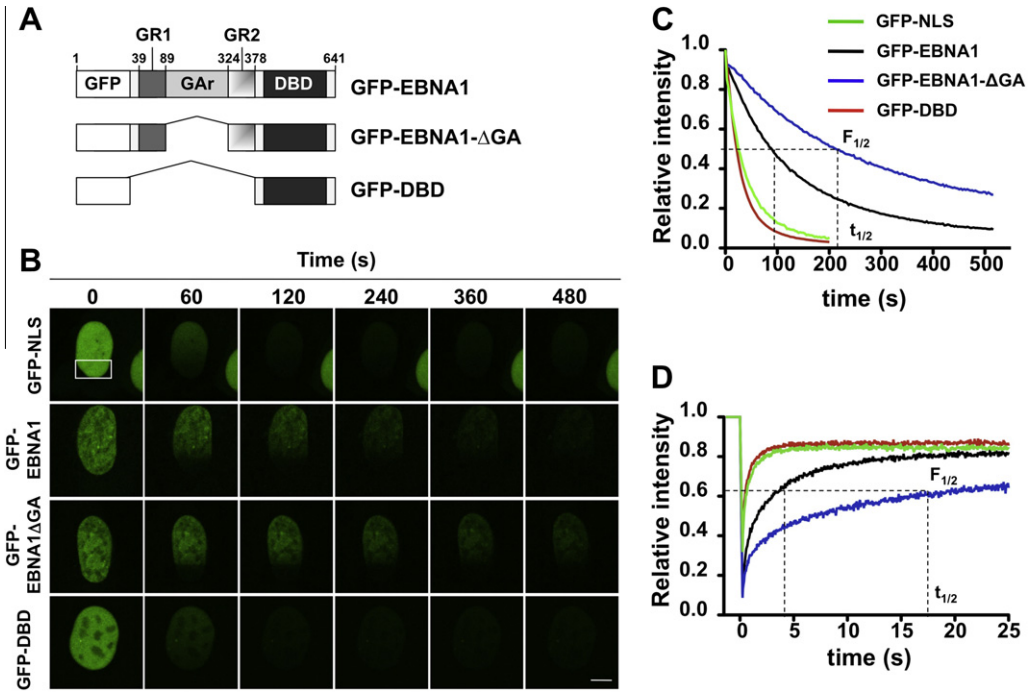

Fig. 3. The Gly–Ala repeats modulate the interaction of EBNA1 with cellular chromatin. (A) Schematic illustration of EBNA1 showing the two Gly–Arg rich domains (GR1 and GR2) separated by the Gly–Ala repeat (GAr) and the C-terminal viral episome binding domain (DBD). The mobility of EBNA1, EBNA1ΔGA and EBNA1-DBD was compared in transfected U2OS cells by FLIP and FRAP analysis. (B) Representative micrographs illustrating the loss of GFP fluorescence in FLIP assays. (C) FLIP kinetics illustrating the decrease mobility of EBNA1 upon deletion of the GAr. The mobility of EBNA-DBD was comparable to that of the soluble GFP-NLS, confirming the failure to interact with cellular chromatin. (D) FRAP kinetics confirming the decreased mobility of EBNA1 upon deletion of the GAr. The $t_{1/2}$ were 4.43 ± 0.1 s and 16.52 ± 0.28 s, respectively.

Table 1
The GA repeat modulates the mobility of EBNA1 on chromatin[a].

Protein	$t_{1/2}$ (seconds)	*t*-test[b]
GFP-NLS	0.26 ± 0.02	
GFP-EBNA1	4.43 ± 0.10	$p < 0.0001$
GFP-EBNA1-ΔGA	16.52 ± 0.28	$p < 0.0001$
GFP-DBD	0.49 ± 0.02	ns

[a] mean ± SE of three independent experiments.
[b] compared with the mobility of GFP-NLS. ns = non significant.

4. Discussion

The results of this study add to the growing body of evidence that highlights the functional significance of the interaction of EBNA1 with cellular chromatin. It is increasingly clear that, in addition to the well-understood role in coordinating the replication of viral and cellular DNA, and tethering of the viral episome to mitotic chromosomes, the interaction of EBNA1 with many different chromatin sites during interphase plays a key role in the cellular remodelling that allows virus persistence and promotes malignant transformation. The expression of EBNA1 is associated with a broad rearrangement of the cellular transcription profile [20], but a direct correlation between binding of EBNA1 and the regulation of cellular promoters has been confirmed only in few cases [15,21]. This apparent discrepancy has several possible explanations but one interesting scenario is suggested by the finding that EBNA1 is a highly mobile protein and resembles, in this respect, the High Mobility Group (HMG) family of architectural transcription factors. The rapid diffusion of HMGs on interphase chromatin is a key determinant in their capacity to decrease the compactness of chromatin through displacement of linker histones [12], which allows the binding of a broad variety of regulators that exert both positive and negative effects on transcription. Indeed, the chromatin-targeting module of EBNA1 resembles the AT-hook of HMGA proteins and we have recently shown that the two proteins share the capacity to promote chromatin decompaction with a slow kinetics, without recruitment of ATP-dependent remodelers and with concomitant mobilization of histone H1 [18].

Here we have found that EBNA1 is less mobile on mitotic chromosomes compared to interphase chromatin (Fig. 2). This observation is in agreement with the recent report of Jourdan et al. [16] who attributed their findings to the capacity of EBNA1 to interact with chromatin binding proteins such as HMGB2 and possibly others. While the involvement of cofactors is a likely explanation for the decreased mobility of EBNA1 during mitosis, the possibility that post-translational modifications may regulate the interaction of EBNA1 with DNA or with various DNA-binding proteins in a cell-cycle dependent manner remains an interesting focus for future research.

Based on FRAP kinetics in HeLa cells expressing GFP-EBNA1, Jourdan et al. reported a diffusion rate of approximately 19 s in interphase cells, with a significant proportion of the protein being immobile. In contrast, we recorded a considerably faster diffusion of GFP-EBNA1 in transfected U2OS and EBV positive C666-1 cells, with a $t_{1/2}$ recovery of approximately 4 s during interphase and apparently no immobile fraction (Fig. 1 and Table 1). This discrepancy is likely to be explained by the absence of the GAr from the EBNA1 construct used by Jourdan et al. Indeed, deletion of the GAr from our constructs significantly reduced the mobility of EBNA1 and caused the appearance of a slow or possibly immobile fraction (Fig. 3 and Table 1). It is noteworthy that a four-fold decrease of diffusion rate could have important functional consequences by decreasing the capacity of EBNA1 to compete for temporarily vacant linker histone binding sites, hampering thereby the chromatin remodelling function.

Collectively, these observations point to the peculiar architecture of the chromatin-targeting module of EBNA1 as a critical determinant for its activity. Indeed, using a set of chimeric proteins containing GFP fused to different combinations of the structural elements present in EBNA1, we have found that both the GR1 and GR2 domains are required for efficient tethering to chromatin

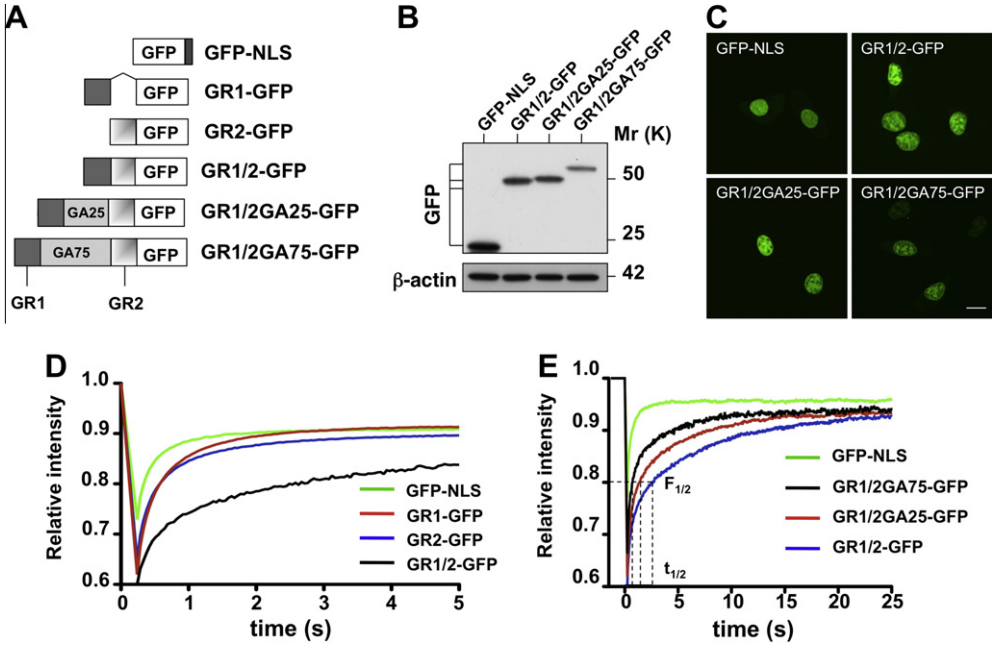

Fig. 4. The mobility of EBNA1 is regulated by GR1 and GR2 domains and by the length of the GAr. (A) Schematic illustration of the GFP chimeras generated by fusion of the GR1 or GR2 alone, or the GR1 and GR2 without or with intervening GAr peptides of 25 or 75 amino acids. (B) Representative western blot illustrating the expression of polypeptides of the expected size in transfected U2OS cells. (C) Representative micrographs illustrating the nuclear localization of the GFP chimeras. (D) FRAP analysis illustrating the requirement of both the GR1 and GR2 modules for efficient chromatin retention. Each module alone induced a small retardation of fluorescence recovery compared to NLS-GFP. (E) FRAP analysis illustrating the length-dependent effect of the GAr on protein mobility.

Table 2
Mobility is modulated by the length of the intervening GAr[a].

Protein	$t_{1/2}$ (seconds)	*t*-test[b]
GFP-NLS	0.26 ± 0.02	
GR1/2-GFP	3.54 ± 0.10	$p < 0.001$
GR1/2GA25-GFP	2.46 ± 0.07	$p < 0.001$
GR1/2GR75-GFP0	1.23 ± 0.07	$p < 0.001$

[a] mean ± SE of three independent experiments.
[b] compared to the mobility of GFP-NLS.

(Fig. 4D) while the intervening GAr regulates the diffusion property in a length dependent manner (Fig. 4E and Table 2). The requirement for both the GR1 and GR2 is in agreement with functional data demonstrating that both domains are required for the episome maintenance function of EBNA1, and is also in line with our previous finding that only in the presence of both domains the binding becomes resistant to detergent extraction and capable of confer resistance to proteasomal degradation [14]. The effect of the GAr on protein mobility is particularly interesting since it illustrates a previously unrecognized mechanism by which this protein domain could regulate the function of EBNA1. It is important to notice that, although dispensable for the capacity of the virus to immortalize B-lymphocytes *in vitro*, the GAr is present in all EBV isolates, and is conserved in the EBNA1 homologs encoded by other lymphocryptoviruses. The length of the repeat is also likely to be important *in vivo* since, although the size varies in different isolates, shortest documented repeats are at least 50–60 amino acids long. Based on our findings, this may be the minimal length required to significantly affect the diffusion properties of EBNA1.

Acknowledgments

We thank E. Kieff, J. Middeldorp, H. van Hattikum, for the kind gift of reagents, plasmids and cell lines. This study was supported by grants awarded by the Swedish Cancer Society, the Swedish Medical Research Council and the Karolinska Institutet, Stockholm, Sweden. NM was supported by a fellowship of the Pakistan government.

References

[1] A.B. Rickinson, E. Kieff, Epstein–Barr virus, in: B.N. Fields, D.M. Knipe, P.M. Howley (Eds.), Virology, Lippincott-Raven, Philadelphia, 1996, pp. 2397–2446.
[2] E. Kieff, Epstein–Barr virus and its replication, in: B.N. Fiels, D.M. Knipe, P.M. Howley, et al. (Eds.), Fields Virology, third ed., Lippincott, Raven Publishers, Philadelphia, 1996, pp. 2343–2396.
[3] E.R. Leight, B. Sugden, EBNA-1: a protein pivotal to latent infection by Epstein–Barr virus, Rev. Med. Virol. 10 (2000) 83–100.
[4] J. Yates, N. Warren, D. Reisman, B. Sugden, A cis-acting element from the Epstein–Barr viral genome that permits stable replication of recombinant plasmids in latently infected cells, Proc. Natl. Acad. Sci. USA 81 (1984) 3806–3810.
[5] D. Mackey, B. Sugden, The linking regions of EBNA1 are essential for its support of replication and transcription, Mol. Cell. Biol. 19 (1999) 3349–3359.
[6] V. Marechal, A. Dehee, R. Chikhi-Brachet, T. Piolot, M. Coppey-Moisan, J.C. Nicolas, Mapping EBNA-1 domains involved in binding to metaphase chromosomes, J. Virol. 73 (1999) 4385–4392.
[7] J. Sears, M. Ujihara, S. Wong, C. Ott, J. Middeldorp, A. Aiyar, The amino terminus of Epstein–Barr Virus (EBV) nuclear antigen 1 contains AT hooks that facilitate the replication and partitioning of latent EBV genomes by tethering them to cellular chromosomes, J. Virol. 78 (2004) 11487–11505.
[8] K. Falk, J.W. Gratama, M. Rowe, J.Z. Zou, F. Khanim, L.S. Young, M.A. Oosterveer, I. Ernberg, The role of repetitive DNA sequences in the size variation of Epstein–Barr virus (EBV) nuclear antigens, and the identification of different EBV isolates using RFLP and PCR analysis, J. Gen. Virol. 76 (Pt 4) (1995) 779–790.
[9] Y. Yin, B. Manoury, R. Fahraeus, Self-inhibition of synthesis and antigen presentation by Epstein–Barr virus-encoded EBNA1, Science 301 (2003) 1371–1374.
[10] J. Levitskaya, M. Coram, V. Levitsky, S. Imreh, P.M. Steigerwald-Mullen, G. Klein, M.G. Kurilla, M.G. Masucci, Inhibition of antigen processing by the internal repeat region of the Epstein–Barr virus nuclear antigen-1, Nature 375 (1995) 685–688.
[11] R. Reeves, Molecular biology of HMGA proteins: hubs of nuclear function, Gene 277 (2001) 63–81.
[12] F. Catez, H. Yang, K.J. Tracey, R. Reeves, T. Misteli, M. Bustin, Network of dynamic interactions between histone H1 and high-mobility-group proteins in chromatin, Mol. Cell. Biol. 24 (2004) 4321–4328.
[13] S.C. Hung, M.S. Kang, E. Kieff, Maintenance of Epstein–Barr virus (EBV) oriP-based episomes requires EBV-encoded nuclear antigen-1 chromosome-binding domains, which can be replaced by high-mobility group-I or histone H1, Proc. Natl. Acad. Sci. USA 98 (2001) 1865–1870.
[14] G. Coppotelli, N. Mughal, D. Marescotti, M.G. Masucci, High avidity binding to DNA protects ubiquitylated substrates from proteasomal degradation, J. Biol. Chem. 286 (2011) 19565–19575.
[15] F. Lu, P. Wikramasinghe, J. Norseen, K. Tsai, P. Wang, L. Showe, R.V. Davuluri, P.M. Lieberman, Genome-wide analysis of host-chromosome binding sites for Epstein–Barr virus nuclear antigen 1 (EBNA1), J. Virol. 7 (2010) 262.
[16] N. Jourdan, A. Jobart-Malfait, G. Dos Reis, F. Quignon, T. Piolot, C. Klein, M. Tramier, M. Coppey-Moisan, V. Marechal, Live-cell imaging reveals multiple interactions between Epstein–Barr virus nuclear antigen 1 and cellular chromatin during interphase and mitosis, J. Virol. 86 (2012) 5314–5329.
[17] M.S. Luijsterburg, C. Dinant, H. Lans, J. Stap, E. Wiernasz, S. Lagerwerf, D.O. Warmerdam, M. Lindh, M.C. Brink, J.W. Dobrucki, J.A. Aten, M.I. Fousteri, G. Jansen, N.P. Dantuma, W. Vermeulen, L.H. Mullenders, A.B. Houtsmuller, P.J. Verschure, R. van Driel, Heterochromatin protein 1 is recruited to various types of DNA damage, J. Cell Biol. 185 (2009) 577–586.
[18] G. Coppotelli, N. Mughal, S. Callegari, R. Sompallae, L. Caja, M.S. Luijsterburg, N.P. Dantuma, A. Moustakas, M.G. Masucci, The Epstein–Barr virus nuclear antigen-1 reprograms transcription by mimicry of High Mobility Group A proteins, Nucl. Acids Res. 2013, http://dx.doi.org/10.1093/nar/gkt032.
[19] D. Martorelli, G. Coppotelli, E. Muraro, R. Dolcetti, M.G. Masucci, Remodeling of the epitope repertoire of a candidate idiotype vaccine by targeting to lysosomal degradation in dendritic cells, Cancer Immunol. Immunother. 61 (2011) 881–892.
[20] R. Sompallae, S. Callegari, S.A. Kamranvar, M.G. Masucci, Transcription profiling of Epstein-Barr virus nuclear antigen (EBNA)-1 expressing cells suggests targeting of chromatin remodeling complexes, PLoS ONE 5 (2010) e12052.
[21] L.R. Dresang, D.T. Vereide, B. Sugden, Identifying sites bound by Epstein-Barr virus nuclear antigen 1 (EBNA1) in the human genome: defining a position-weighted matrix to predict sites bound by EBNA1 in viral genomes, J. Virol. 83 (2009) 2930–2940.